

Optical response of small carbon clusters

K. Yabana¹, G.F. Bertsch²

¹ Department of Physics, Niigata University, Niigata, Japan

² Physics Department and Institute for Nuclear Theory, University of Washington, Seattle, WA 98195, USA (e-mail: bertsch@phys.washington.edu)

Received: 13 May 1997 / Final version: 25 August 1997

Abstract. We apply the time-dependent local density approximation (TDLDA) to calculate dipole excitations in small carbon clusters. A strong low-frequency mode is found which agrees well with observation for clusters C_n with n in the range 7–15. The size dependence of the mode may be understood simply as the classical resonance of electrons in a conducting needle. For a ring geometry, the lowest collective mode occurs at about twice the frequency of the collective mode in the linear chain, and this may also be understood in simple terms.

PACS: 22.8.97

I Introduction

In this work we examine strong optical transitions in light carbon clusters, with the goal of providing a diagnostic tool for the structure of the clusters. Carbon has a rather complex structural evolution [1] as a function of the number of atoms n . Small clusters are linear, and at higher n rings are favored. For intermediate n values, rings may be more favored at even n and linear chains at odd n . Direct information on the shapes of the clusters may be obtained by ion chromatography [2], but one mostly relies on spectroscopic data to interpret the structure [3].

We will demonstrate that the strong optical absorption resonances behave in a very systematic way as function of cluster size, and that the frequency of the transitions gives direct information about the shape of the cluster. In particular, the strong $\pi - \pi^*$ transition in chains is at about half the frequency of the mode in rings. We also find that the frequencies can be understood very simply using classical concepts. The most important determinant in systems of similar composition is the polarizability, which is much larger for chains along their axes than for rings in the plane of the ring.

In the Sect. 2 below we discuss our quantum calculations, which are done using the time-dependent local-density approximation (TDLDA). This is nothing more than the Kohn-Sham equations with the “energy” of the orbital replaced by

the time derivative $i\partial/\partial t$. The TDLDA and its small amplitude limit has been shown to be a reliable tool to calculate strong resonances in the optical response of metallic clusters [4, 5] and molecules such as C_{60} [6] and polyenes [7]. Our method to solve the equations is a very straightforward one, but it deserves some discussion because there are many implementations of small-amplitude TDLDA in the literature, and our method is not conventional in condensed-matter or chemical physics. We use a Hamiltonian of the usual Kohn-Sham form, taking a local-density approximation for the non-Coulombic electron-electron interaction, and a pseudopotential to describe the carbon ions.

However, the calculations with *ab initio* Hamiltonians are very time consuming, and it is important to analyze the results to gain understanding of the functional dependence of the excitation energy on the cluster properties. This will be done in Sect. 3; our result briefly is that the resonance frequency ω_n in chains scales with n as $\omega_n \propto \sqrt{\ln n}/n$. This applies to both chains and rings, with different coefficients of proportionality.

Part of the interest in the spectra of carbon chains comes from astrophysics, the question of the composition of interstellar matter. Absorption bands are seen which may be due to carbon clusters, but specific identification of species remains controversial [8, 9]. The TDLDA is probably only reliable to 10% or so on the frequencies of the strong transitions, which is not enough to use the theory to assign unknown transitions. However, it might be that the theory could be used to predict the shifts due to small changes in structure, for example by adding another atom at the end of the chain. We plan in the future to investigate various molecules that are similar to the carbon chains and see how large the perturbations are.

II TDLDA

A General

Time-dependent mean field theory is a powerful tool to calculate the collective excitations of quantum many-particle systems, and it has been widely applied in cluster physics. There are a number of implementations of the theory, all

starting from the time-dependent Schrodinger equation. With the local density approximation for the electron-electron interactions, the equation has the form of a time-dependent Kohn-Sham equation,

$$i\hbar \frac{\partial}{\partial t} \psi_i(\mathbf{r}, t) = \left\{ \frac{\hbar^2}{2m} \nabla^2 + \sum_{a \in \text{ion}} V_{\text{ion}}(\mathbf{r} - \mathbf{R}_a) + e^2 \int d\mathbf{r}' \frac{n(\mathbf{r}', t)}{|\mathbf{r} - \mathbf{r}'|} + V_{xc}(n(\mathbf{r}', t)) \right\} \psi_i(\mathbf{r}, t). \quad (1)$$

Here ψ_i represents a single-particle wave function, $n(\mathbf{r}, t)$ is the electron density, V_{ion} is the ionic core potential, and V_{xc} is the potential associated with exchange and correlations. For our purposes, ψ_i is not perturbed greatly from the ground state wave function, and a small amplitude approximation justifiable. This leads to the RPA and the linear response method of solution. We believe that for large numbers of particles, the most efficient technique to treat LDA Hamiltonians is the straightforward integration of the time-dependent equations of motion. The argument is given in the Appendix. The optical response of the light chains $C_{3,5}$ and C_7 has been calculated with the configuration-interaction method of quantum chemistry [10, 11], but this brute-force technique is impractical in large clusters.

Our numerical method is taken over from the nuclear physics [12], where it is called the TDHF theory. The efficiency of the method requires that the Hamiltonian matrix be sparse, and this is fulfilled by using a coordinate mesh to represent the wave function. It is also necessary for numerical efficiency to use Hamiltonians whose energy scales are not too large; this means that one treats only valence electrons and uses pseudopotentials for V_{ion} to take into account the effects of the core electrons. Thus we treat dynamically only the four valence electrons of carbon. Our pseudopotentials are calculated according to the commonly accepted prescriptions [13, 14]. The exchange-correlation potential V_{xc} is taken from [15].

Some details of our integration algorithm are given in the Appendix. The important numerical parameters are the spatial mesh size Δx , the number of mesh points M , the time step Δt , and the total length of time integration T . The values for these parameters are discussed below.

B Initial conditions

We wish to start with the Kohn-Sham ground state wave function, and in principle the geometry of the ions as well as the electron wave functions are determined by minimizing the Hamiltonian function. However, a full minimization of the structures is quite time consuming, and we believe that small variations in bond lengths will not have a significant effect on the collective excitations. We therefore take geometries from outside rather than calculating *ab initio*. For simplicity, we fixed the nearest neighbor distance of the carbon atoms at 1.28 Å. This is the average LDA equilibrium distance for large circular rings or long chains.

To calculate the response, our initial wave functions are perturbed from the static solutions ϕ_i by a velocity field

$$\psi_i(\mathbf{r}, 0) = e^{ikz} \phi_i(\mathbf{r}). \quad (2)$$

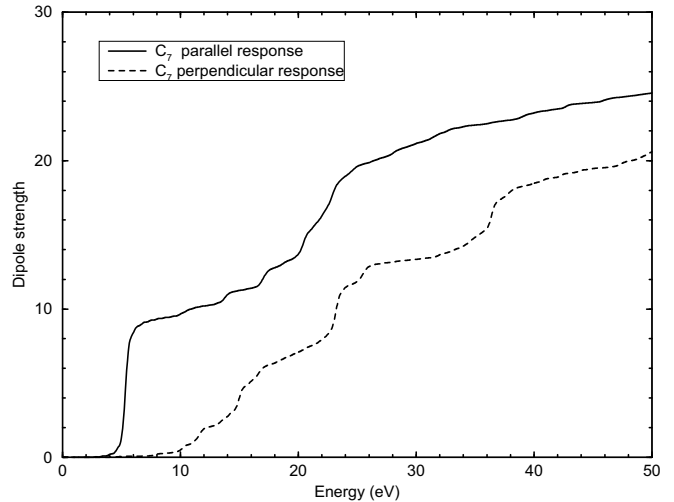


Fig. 1. Optical response of the linear chain C_7 , calculated in TDLDA. The mesh spacing is $\Delta x = 0.3 \text{ \AA}$ and $\Delta t = 0.001 \text{ eV}^{-1}$. The spatial grid has the shape of a cylinder, with 30,000 mesh points. The integration time was 10 eV^{-1}

The momentum k is set to be small to ensure that the response is linear (we use typically $k = 0.1 \text{ \AA}^{-1}$). The real-time evolution of the dipole moment is obtained as

$$z(t) = \sum_i \langle \psi_i(t) | z | \psi_i(t) \rangle, \quad (3)$$

and its Fourier transform in time gives the dipole strength function $S(\omega)$

$$S(\omega) = \frac{2\omega m}{\pi k} \int_0^\infty dt z(t) \sin(\omega t). \quad (4)$$

The strength function defined in this way is related to the oscillator strength f by

$$\int d\omega S(\omega) = f. \quad (5)$$

C Results

We first discuss the numerical parameters needed for carbon clusters. We found that a mesh size of $\Delta x = 0.3 \text{ \AA}$ is needed to adequately represent the *sp*-orbitals of carbon. This is more than a factor of two finer than the mesh size parameter needed for the *s*-orbitals of alkali metals. The wave function is represented on this grid within the interior of a cylindrical volume. The size of the cylinder is chosen to include all mesh points within 4 \AA of each carbon atom. With this procedure, the wave function for the C_7 cluster requires 30,000 mesh points.

There are two numerical time parameters. The first is the time step in the integration. In the carbon calculations we used $\Delta t = 0.001 \text{ eV}^{-1}$, which is an order of magnitude smaller than the value needed for alkali metal clusters. This corresponds to the order-of-magnitude difference between the maximum kinetic energies in the meshes used for systems, 0.3 \AA in carbon versus 0.8 \AA in alkali metals. The other numerical time parameter is the total integration time T . The inverse of this sets the scale for the energy resolution in the response; we use $T = 10 \text{ eV}^{-1}$ to make visible structure on the energy scale of 0.1 eV .

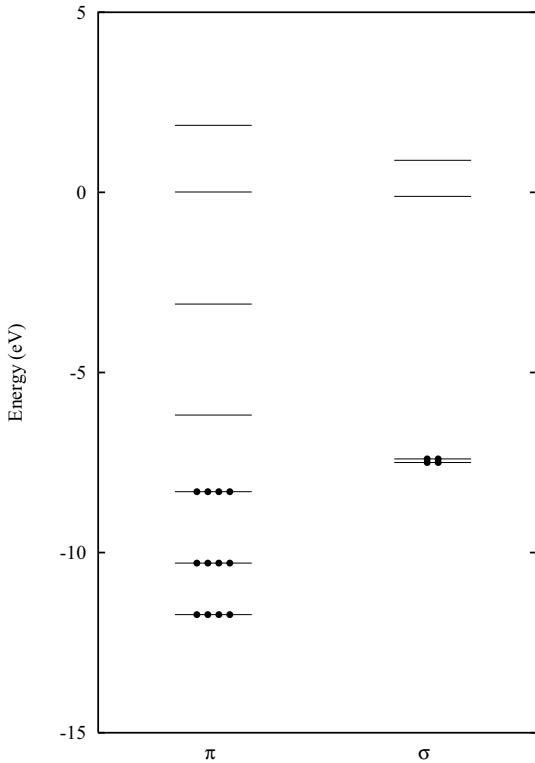


Fig. 2. Molecular orbital diagram for the C_7 chain in the LDA. On the left are shown the lowest π states, which correspond to the 7 orbitals of the tight-binding approximation. On the right are the highest occupied and lowest unoccupied σ orbitals

The response of a typical case, C_7 , is shown in Fig. 1. Plotted is the integrated oscillator strength as a function of excitation energy. The upper curve shows the response parallel to the chain, and the lower curve shows the perpendicular response. The total sum rule ($f = 4n = 28$, four valence electrons per carbon atom), is satisfied to within 10% by the calculation¹ The longitudinal response has a strong excitation¹ The longitudinal response has a strong excitation at 5.3 eV. About 1/3 of the 28 units of oscillator strength is in this excitation. The perpendicular response has no corresponding strong excitation below 10 eV. The small wiggles in the calculated response are artifacts of the truncation in the Fourier transformation. In our case here, the effect is obviously small. To understand better the nature of the 5.3 eV collective excitation, it is helpful to know the characteristics of the orbitals near the Fermi surface and the corresponding single-particle transitions. The single-particle level scheme, giving by the eigenenergies of the static Hamiltonian, are shown in Fig. 2. The lowest strong single-particle transition is between the highest occupied and lowest empty π orbitals. This gap is 2.1 eV, roughly half the frequency of the TDLDA mode. Note that there are two σ orbitals within the $\pi - \pi^*$ gap, but these electrons are localized on the outer ends of the carbon chain and do not couple strongly to the other states.

The 2.1 eV $\pi - \pi^*$ transition has a very large oscillator strength ($f = 10.2$), which equals the strength of the TDLDA

¹ In principle, the TDLDA conserves the sum rule exactly if the Hamiltonian is local. This is not the case when the core electrons are omitted, because the resulting pseudopotentials have a nonlocal character [14]

Table 1. Excitation energy and strength of carbon chains in TDLDA

Size	E_{free} [eV]	f_{free}	E_{TDLDA} [eV]	f_{TDLDA}
3	4.15	3.5	8.1	3.1
4	3.89	5.2	7.2	4.5
5	2.81	6.9	6.4	6.3
6	2.72	8.6	5.9	8.0
7	2.13	10.2	5.3	9.8
8	2.10	11.9	5.0	11.4
9	1.71	13.5	4.6	13.1
10	1.71	15.2	4.4	14.8
11	1.43	16.7	4.1	16.4
12	1.44	18.4	3.9	18.1
13	1.23	19.8	3.7	19.7
14	1.26	21.6	3.5	21.3
15	1.08	22.9	3.3	22.9
20	0.90	31.7	2.7	30.8

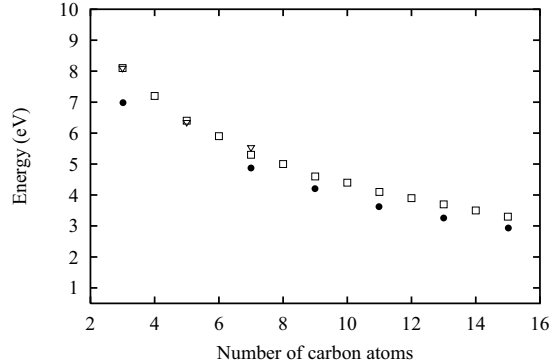


Fig. 3. Systematics of the longitudinal mode in C_N linear chains. Filled circles: experimental, from [18] and [16]; squares, TDLDA; triangles, quantum chemistry calculations from [10] and [11]

mode to within 4%. The magnitude of f may be understood qualitatively as equal to the number of π electrons. To a good approximation, the longitudinal dipole operator on π electrons in a chain keeps them in the π manifold, so the sum rule is approximately conserved within the π manifold. The number of them in an odd- n chain is $N = 2n - 2$, filling the molecular orbitals in the usual way. Thus, if the lowest transition would exhaust the sum rule, the oscillator strength would be $f = 12$ for the twelve π electrons in C_7 . This is to be compared with ~ 10 from the LDA wave functions.

We have calculated the excitation energies and oscillator strengths for the collective transition for carbon chains in the range² $N = 3 - 20$, and the results are tabulated in Table 1. When more than one transition is seen, the average excitation energy and the summed oscillator strength are given. The features described for C_7 apply systematically these chains. The oscillator strength is roughly given by the number of π electrons; the frequency of the TDLDA mode is larger than the unperturbed excitation energy by a factor that ranges from 2 in the light chains to 3 in the heavier ones. The frequencies from Table 1 are graphed in Fig. 3 and one can see that they vary smoothly with chain length. The filled circles are experimental points for odd n from [16] and [18]. We see rather good agreement for the larger

² In the ground state of the even- n clusters with chain geometry, the highest occupied orbital is doubly degenerate and we assumed each spatial orbital to be occupied by one electron to make a triplet ground state. For other cases, all the occupied orbitals are completely filled

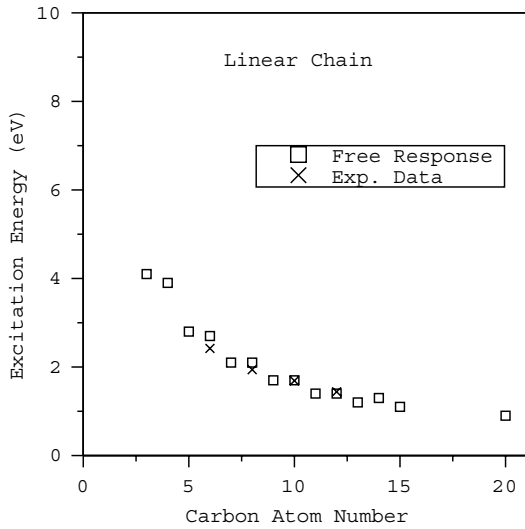


Fig. 4. Systematics of $\pi - \pi^*$ gap energies compared with observed transitions from [19, 20]

Table 2. Excitation energy and strength of carbon rings in TDLDA

Size	E_{free} [eV]	f_{free}	E_{TDLDA} [eV]	f_{TDLDA}
7	4.9	5.8	7.8	3.1
8	4.8	8.6	8.2	4.6
9	4.1	9.0	7.6	5.5
10	3.7	9.8	7.2	6.9
11	3.5	10.7	7.0	7.9
12	3.3	11.8	6.9	9.2
13	3.0	12.5	6.6	10.3
14	2.8	13.5	6.3	11.3
15	2.6	14.4	6.1	12.4
20	2.0	18.7	5.2	17.4

chains. The clusters $C_{3,5,7}$ have been calculated by the CI method of quantum chemistry [11], and the predicted strong transition is in the same region, at 8.10, 6.35, and 5.54 eV, respectively, which are close to our results of 8.1, 6.4, and 5.3 eV. The oscillator strength for C_3 is calculated in [11] as about 1.1. The oscillator strength given in Table 1 is 3.1 for C_3 , but this is the strength along the chain direction. Dividing the strength by three to average over spatial orientations gives $f=1.0$, in agreement with the quantum chemistry calculation. While there is experimental data for the excitation energies of odd- n chains in the range $n = 7 - 15$, there is no corresponding data on the even chains. We are confident that the systematics is smooth going over odd and even n , so it should be possible to observe the mode in even- n .

Reference [18] also reported weaker transitions in odd- n chains at lower energy. The authors in [19, 20] observe transitions in heavier even- n clusters which fall within the same systematics as the weak odd- n transitions. We believe that the even- n transitions may be associated with the single-particle transition across the energy gap. There are two inequivalent electrons at the Fermi surface due to the partial orbital occupancy, and one combination becomes the high-frequency collective state and the other combination remains near the gap energy with only a small oscillator strength. In Fig. 4 we show the systematics of the low transition, compared to the calculated $\pi - \pi^*$ gap energy.

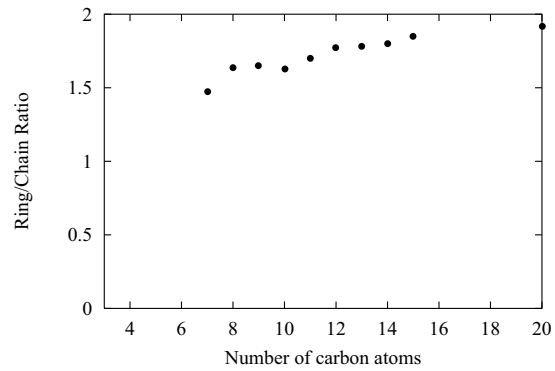


Fig. 5. Ratio of the collective excitation energy in rings with compared to chains, from the TDLDA

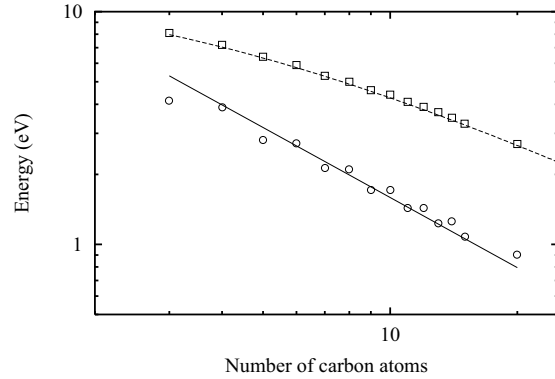


Fig. 6. Systematics of the single-electron transition and the collective excitation in chains, compared with functional fits of the form (6) and (7)

We have also calculated the in-plane response of ring configurations in the range $N = 7 - 15$. For simplicity we assumed uniform circular rings, although the structures may have some distortion [21]. The results for the collective π transition are shown in Table 2. The ratio of collective frequencies for rings to chains is plotted in Fig. 5. We see that the rings are predicted to have a collective frequency about twice that of the chains with the same number of atoms.

III Interpretation

Our goal in this section is to characterize the n -dependence of the excitations, and further the dependence on shape, whether chain or ring. It is well known that the Fermi gap (or HOMO-LUMO gap) $\Delta\epsilon$ in a linear chain depends on n as

$$\Delta\epsilon \propto \frac{1}{n}. \quad (6)$$

This function fits well the systematics of our calculated single-particle transition energy, but it does not describe the collective excitation. This may be seen from the log-log plot of the energies in Fig. 6. The figure shows that electron-electron interaction plays an important role not only in the absolute frequency of the transition but in its functional form as well. The inadequacy of (6) to describe the systematics of the strong excitation was also mentioned in [18].

In purely classical physics, the analogous problem is the plasma resonance in a needle-shaped conductor. The closest

problem that can be treated analytically is plasma resonance in a ellipsoidal conductor. Reference [22] derives the formula,

$$\omega^2 = \frac{1 - e^2}{e^2} \left(-1 + \frac{1}{2e} \log \frac{1+e}{1-e} \right) \omega_0^2 \quad (7)$$

where e is related to the ratio of short to long axes, R_{\perp}/R_{\parallel} , by

$$e^2 = 1 - \left(\frac{R_{\perp}}{R_{\parallel}} \right)^2. \quad (8)$$

This formula has been applied to the collective π excitations in football-shaped fullerenes [23]. For our problem, we obtain the fit shown in Fig. 6, treating ϵ and ω_0 as adjustable parameters. It describes the systematics very well. Of course, the carbon chain is not ellipsoidal, and we should seek rather that analytic behavior of the resonance in a conducting cylinder.

The behavior of electromagnetic resonances on infinitely long wires is known from classical electromagnetic theory. The dispersion formula for the one-dimensional plasmon on a long wire reduces to the following expression in the long-wave length, thin wire limit [24, 25].

$$\omega^2 = \frac{4\pi n_e e^2}{m} q^2 \log \frac{1}{qa} \quad (9)$$

where q is the reduced wave number of the plasmon, n_e is the density of electrons per unit length, and a is the radius of the wire. For a finite wire, the lowest mode would have a q varying inversely with the length of the wire L . Thus the lowest mode would behave as

$$\omega \propto \frac{\sqrt{\ln(L)}}{L}. \quad (10)$$

This in fact is the asymptotic behavior of (7) in the limit of large $R_{\parallel} = L$. Taking $L \propto n$, the frequency dependence in chains would be

$$\omega \propto \frac{\sqrt{\ln(n)}}{n} \quad (11)$$

This behavior can be extracted from a more quantum approach using the polarizability estimate of the collective frequency [26],

$$\omega^2 = \frac{\hbar^2 e^2 N}{m\alpha}. \quad (12)$$

Here N is the number of active electrons and α is the polarizability. This formula is derived from the ratio of sum rules, and N may be identified with the oscillator strength f associated with the transition. We established in Sect. 2 that the oscillator strength in the π manifold of states is given roughly by the number of π electrons, and scales accordingly with n .

We next estimate the polarizability. The asymptotic behavior for large n can be determined under the assumption that the chain behaves as a perfect conductor. The electrons in a perfect conductor will respond to an external field to restore the internal electric field to zero. This gives an implicit equation for the electron density in terms of the external electric field \mathcal{E} ,

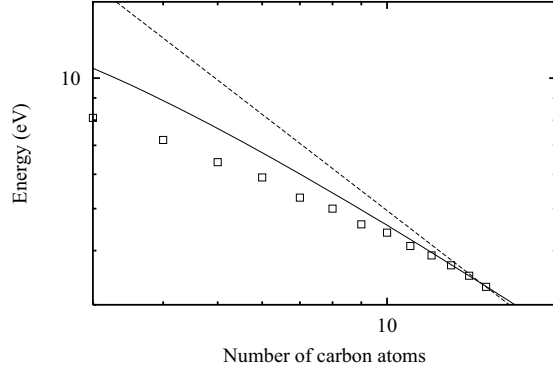


Fig. 7. Comparison of the TDLDA collective excitation in chains with (6) and (11)

$$z\mathcal{E} = e \int dz' \delta n(z') V(z - z') \quad (13)$$

Here $\delta n(z)$ is the induced linear electron density, obtained by integrating the induced ordinary density over transverse coordinates. If this is solved for $\delta n(z)$, the polarizability is then obtained as the ratio of the induced dipole moment to \mathcal{E} ,

$$\alpha = \frac{1}{\mathcal{E}} \int dz' z' \delta n(z'). \quad (14)$$

To determine asymptotic behavior, we note that $V(z)$ is strongly peaked at zero, so we may approximate it as a δ function times $\int V dz$:

$$\int dz' \delta n(z') V(z - z') \approx \delta n(z) \int dz' V(z') \quad (15)$$

The $V(z)$ behaves as $1/|z - z'|$ at large separation, so the integral on the right hand side depends logarithmically on the integration limits. Thus we may estimate the integral as

$$\int dz' V(z') \approx \int_{-L/2}^{L/2} dz' V(z') \approx 2 \log\left(\frac{L}{a}\right). \quad (16)$$

Here a is a length having the order of magnitude of the transverse dimension of the wire. We thus obtain

$$\delta n(z) \approx \frac{z\mathcal{E}}{2 \log(L/a)}. \quad (17)$$

From (4), this implies that the polarizability is

$$\alpha = \frac{L^3}{24 \log(L/a)} \quad (18)$$

We now insert this in (12) and use $n \sim L$ to obtain (11). The fit with this function is shown in Fig. 7. It obviously describes the asymptotic behavior much better than (6), which is also shown in the figure.

We finally discuss the relative frequencies of the modes in chains and rings using (12). We first examine the oscillator strengths, needed for the numerator of (12). Naively we would expect similar values, since the number of π electrons in a ring from orbital counting is given by $N = 2n$. However, comparing Tables 1 and 2, we may see that the in-plane ring values are only 2/3 the chain values along the

axes³. Much more important for the frequency change is the differing polarizabilities of chains and rings. We have made a similar asymptotic estimate of the ring polarizability, and we find that it also increases logarithmically with the circumference of the ring. The ratio of polarizabilities of a thin wire ring compared to a straight wire of the same length is about a factor of 6. The two factors of the oscillator strength ratio and the polarizability ratio combine in (12) to produce a frequency shift by a factor of two. This is indeed what the TDLDA gives asymptotically (see Fig. 5), confirming the polarizability and oscillator strength argument we made here.

IV Conclusion

We have demonstrated that the collective π transition in carbon chains and rings behaves in a very systematic way, calculable to $\approx 10\%$ accuracy by TDLDA, and understandable in macroscopic terms. This should give one confidence in using these transitions to infer the shape of the clusters. We hope in addition that the smooth dependence of the transition would allow its perturbation going between similar structures to be calculable to accuracy of interest for spectroscopic identification purposes.

We thank R.A. Broglia for calling our attention to (7). This work is supported by the Department of Energy under Grant No. DE-FG06-90ER40561, and by a Grant in Aid for Scientific Research (No. 08740197) of the Ministry of Education, Science and Culture (Japan). Numerical calculations were performed on the FACOM VPP-500 supercomputer in RIKEN and the Institute for Solid State Physics, University of Tokyo.

Appendix: numerical aspects

The method we use, explicit time integration of (1) in the coordinate space representation, can be shown to be the most efficient of the methods in use for large systems when there are no symmetries to reduce the dimensionality. The coordinate space representation is also the most efficient for the static problem under similar conditions [27].

Let us first consider the matrix RPA in a particle-hole configuration space representation. This method has been applied to sodium clusters in [28] and to C_{60} in [6]. The number of numerical operations to extract the eigenmodes and eigenfrequencies scales with the dimensionality of the matrix M as M^3 . The dimensionality of the matrix is given by the number of particle-hole configurations. A complete calculation, guaranteed to respect the sum rules and conservation laws, requires that all occupied and unoccupied orbitals be included in the space. The single-particle space will have a dimensionality that is proportional to the size of the system, and the number of unoccupied orbitals will thus be proportional to the number of particles N . Thus the dimensionality with this method scales as $O(N^6)$. Note that

³ The reason for the lower value is that the electric field in the plane of the ring is partly transverse and partly longitudinal with respect to the C-C bond axes. This implies dipole excitations lie partly outside the π manifold of states. Thus part of the sum rule is shifted to higher energy excitations

this could be much reduced by truncating the particle-hole basis. For example, in our study of collective π transition in carbon chains, the orbitals away from the Fermi energy are not so important. However, we do not know a systematic scheme for truncation that would preserve the oscillator strength and lead to a more favorable N dependence for the algorithm.

Another widely used technique is the linear response method. This has been applied to the molecule N_2 in [29] and to alkali metal clusters in [5]. Here the object one calculates is the density-density response function. In a coordinate space representation, its dimensionality is the number of points in the coordinate space mesh. Thus the dimensionality of the matrix scales as $M \propto N$. The matrix operation required in this case is inversion rather than diagonalization, but it also goes as the cube of the dimension. So this method scales as $O(N^3)$. Note that we could have used another representation of the response, such as momentum space, and still obtained $O(N^3)$ scaling.

The advantage of direct coordinate space methods is that one can take advantage of the sparse character of the Hamiltonian in that representation. The Hamiltonian has a dimensionality that scales $M \propto N$, and the number of operations required to apply the Hamiltonian to a single-particle wave function is also $O(N)$ because of the sparseness. Performing the operation on all N particles is then $O(N^2)$, and this gives the scaling for the method. Note that there is a large prefactor, because the equations have to be integrated many time steps. However, the time integration depends only on the energy scales in the Hamiltonian which does not change with N . Finally, we note that the advantage of this method would apply to any representation of the wave function that allows a sparse Hamiltonian matrix.

For the numerical aspects of integrating the Kohn-Sham equation, we follow closely the method used in [12] to solve the time-dependence mean field equations in nuclear physics. The algorithm must insure energy conservation and norm conservation to very high accuracy to be useful. In addition, for the results to be converged, the time step of the integration must be small compared to the inverse frequencies of the density oscillations. Fixing the time step by this criterion, energy conservation is achieved by using an implicit method to integrate the equations. One can show that the integration over the time step will conserve energy if the mean field is computed with a fixed density given by the average of the initial and final densities, for Hamiltonians with ordinary two-body interactions⁴. In our computer program, we obtain sufficient accuracy for our time steps by using a simple predictor corrector method to find the average density and integrate over the time step.

We have now reduced the problem to the time integration of a fixed Hamiltonian. Since the Schroedinger equation is

⁴ A more general condition, valid for nonlinear density dependencies such as in the correlation-exchange potential, is given by taking the potential in the single-particle Hamiltonian as

$$V(r) = \frac{v[n_+(r)] - v[n_-(r)]}{n_+ - n_-}$$

where v is the potential energy functional of density and n_{\pm} are the densities at the beginning and end of the time step

linear, we can integrate straightforwardly by using the Taylor series expansion of the time evolution operator,

$$\phi(t + \Delta t) = e^{-iH\Delta t}\phi(t) = \sum_{n=0}^{k_{max}} \frac{1}{n!} (iH\Delta t)^n \phi(t) \quad (19)$$

We found that the fourth-order approximant, $k_{max} = 4$, is sufficient with our time steps to insure norm conservation to the needed accuracy.

References

1. W. Weltner, R.J. Van Zee, Chem. Rev. **89**, 1713 (1989)
2. G. von Helden, et al., Chem. Phys. Lett. **204**, 15 (1993)
3. S. Yang et al., Chem. Phys. Lett. **144**, 431 (1988)
4. K. Yabana, G.F. Bertsch, Phys. Rev. **B54**, 4484 (1996)
5. A. Rubio, J.A. Alonso, X. Blase, L.C. Balbas, S.G. Louie, Phys. Rev. Lett. **77**, 247 (1996)
6. C. Yannouleas, E. Vigezzi, J.M. Pacheco, R.A. Broglia, Phys. Rev. **B47** (1993) 9849; F. Alasia et al., J. Phys. **B27**, L643 (1994)
7. Y. Luo, H. Agren, S. Stafstrom, J. Phys. Chem. **98**, 7782 (1994)
8. J. Fulara et al., Nature **366**, 439 (1993)
9. J.K.G. Watson, Astrophys. J. **437**, 678 (1994)
10. G. Pacchioni, J. Koutecky, J. Chem. Phys. **88**, 1066 (1988)
11. M. Kolbuszewski, J. Chem. Phys. **102**, 3679 (1995)
12. H. Flocard, S. Koonin, M. Weiss, Phys. Rev. **C17**, 1682 (1978)
13. N. Troullier, J.L. Martins, Phys. Rev. **B43**, 1993 (1991)
14. L. Kleinman, D. Bylander, Phys. Rev. Lett. **48**, 1425 (1982)
15. J. Perdew, A. Zunger, Phys. Rev. **B23**, 5048 (1981)
16. K. Chang, W. Graham, J. Chem. Phys. **77**, 4300 (1982)
17. D. Forney et al., J. Chem. Phys. **104**, 4954 (1996)
18. D. Forney et al., J. Chem. Phys. **104**, 4954 (1996)
19. P. Freivogel et al., J. Chem. Phys. **103**, 54 (1995)
20. D. Forney et al., J. Chem. Phys. **103**, 48 (1995)
21. K. Raghavachari, J.S. Binkley, J. Chem. Phys. **87**, 2191 (1987)
22. C.F. Bohrn, D.R. Huffman, Absorption and scattering of light by small particles. Wiley, NY, 1983, (5.33)
23. H.E. Roman et al., Chem. Phys. Lett. **251**, 111 (1996)
24. A. Gold, A. Ghazali, Phys. Rev. **B41**, 7632 (23a) (1990)
25. Q.P. Li, S. Das Sarma, Phys. Rev. **B43**, 11768 (2.13) (1991)
26. W. de Heer, Rev. Mod. Phys. **65**, 611 (1993)
27. J.L. Martins, Z. Phys. **D12**, 347 (1989)
28. V. Bonacic-Koutecky, P. Fantucci, J. Koutesky, Chem. Rev. **91**, 1035 (1991)
29. C. Jamorski, M.E. Casida, D.R. Salahub, J. Chem. Phys. **104**, 5134 (1996)